LA-10067-MS

Los Alamos National Laboratory is operated by the University of California for the United States Department of Energy under contract W-7405-ENG-36.

Well Log Interpretation of Certain Geothermal Fields in the Imperial Valley, California

Los Alamos
Los Alamos National Laboratory
Los Alamos, New Mexico 87545

This work was supported by the US Department of Energy, Division of Geothermal and Hydropower Technologies.

Edited by Glenda Ponder and Marge Wilson, ESS Division

GL04001

LA-10067-MS

UC-66b
Issued: March 1984

Well Log Interpretation of Certain Geothermal Fields in the Imperial Valley, California

Iraj Ershaghi*
Doddy Abdassah*

*Department of Petroleum Engineering, University of Southern California, University Park, Los Angeles, CA 90089.

Los Alamos Los Alamos National Laboratory
Los Alamos, New Mexico 87545

CONTENTS

ABBREVIATIONS AND SYMBOLS

CNFD	Compensated neutron/formation density
C_o	Conductivity of brine-saturated rock, mho cm^{-1}
C_w	Conductivity of formation brine, mho cm^{-1}
DIL	Dual induction Laterolog
F	Formation resistivity factor
Q_v	Cation exchange capacity per unit volume, meq/mℓ
R_{ILD}	Resistivity from deep induction log, Ωm
R_{LL8}	Resistivity from Laterolog 8, Ωm
R_{mf}	Mud filtrate resistivity, Ωm
R_w	Formation water resistivity, Ωm
SP	Spontaneous potential, mV
ϕ_D	Density porosity, fraction
ϕ_N	Neutron porosity, fraction
ρ_b	Bulk density, g/cm^3

WELL LOG INTERPRETATION OF CERTAIN GEOTHERMAL FIELDS IN THE IMPERIAL VALLEY, CALIFORNIA

by

Iraj Ershaghi and Doddy Abdassah

ABSTRACT

This study reviews the wireline log responses of some geothermal fields in the Imperial Valley, California. The fields under study include the Heber, the East Mesa, the Brawley, and the Westmoreland. The well logs used in the study did not include all the wireline surveys obtained by the operators. The selected well logs obtained under special arrangements with the operators were chosen to maintain the anonymity of specific well locations but are only representative of each area.

Analysis of the well logs indicates that on an individual field basis, the well logs are excellent for correlation purposes. The presence of extremely saline fluids in some fields precludes the monitoring of Q_v (cation exchange capacity per unit volume) profile for detection of hydrothermally altered zones. The producing sections in all the fields are characterized by low porosity and high resistivity.

I. INTRODUCTION

In a recently published report,[1] the results of well log interpretation in the Cerro Prieto geothermal field in Mexico were discussed. In brief, the interpretation work on these logs indicated that the monitoring of the hydrothermal alteration effects on low-temperature clays and the detection of zones with altered clays may serve as a useful exercise in the delineation of target production zones.

This study investigated the application of these findings from Cerro Prieto to the well logs in some of the fields in the Imperial Valley, California. This study would have been more complete if all the wireline logs of the wells drilled in the Imperial Valley had been examined. Unfortunately, only a few well logs were made available; they are listed in

Table I. However, even with the limited amount of wireline logs, some of the findings reported here are significant and warrant further examination by the operators in the area with access to more information.

The well logs included here belong to the Brawley, the Heber, the Westmoreland, and the East Mesa fields. Concurrent with the task of log interpretation, a literature review was conducted to obtain as much information as possible about each field. In the following sections, a brief review of the geological and reservoir data available on individual fields is made, the research steps are outlined, the results of the interpretative work are presented, and finally, these results are compared among the different fields.

II. HYDROTHERMAL GEOTHERMAL FIELDS IN THE IMPERIAL VALLEY

The geothermal fields in the Imperial Valley are part of the Salton Trough. The trough covers an area of 26 000 km^2.[2] The sedimentary column in the trough consists of interbedded alluvial gravels and sands, eolian silts and sands, and lacustrine silts and clays.[3]

TABLE I

LIST OF WELL LOGS

Field	Well	Operator	Well Logs
Brawley	A	Union Oil Co. of California	DIL, CNFD
	B	Union Oil Co. of California	DIL, CNFD
Mesa	6-1	U.S. Bureau of Reclamation	DIL, CNFD
Heber	A	Chevron Resources	DIL, CNFD
	B	Chevron Resources	DIL, CNFD
	C	Chevron Resources	DIL, CNFD
Westmoreland	1	Republic Geothermal	DIL, CNFD
	2	Republic Geothermal	DIL, CNFD
	3	Republic Geothermal	DIL, CNFD
	4	Republic Geothermal	DIL, CNFD

The Imperial Valley is wedge shaped with a flat, alluviated floor. Numerous strike-slip faults of the San Andreas-San Jacinto system control the structure of the valley.[4]

According to a publication by the U.S. Geological Survey,[5] the total thermal energy in the Salton Trough has been estimated at 240 x 10^8 J with an undiscovered potential of another 480 x 10^8 J.

The significant energy potential of these hydrothermal geothermal fields in the Imperial Valley has been the impetus for the extensive exploration and development during the last two decades. Several major fields have been discovered. Figure 1 shows the location of some of the geothermal fields in the Imperial Valley. The depth to the producing zones ranges from 1000 m (Salton Sea) to 5000 m (South Brawley). Power plants currently on line include Magma's binary cycle at East Mesa, Edison's power plant at Brawley, and the ones at Salton Sea and Niland. Based on detailed studies of the cores and drill cuttings, indications are that the sediments are at various stages of diagenesis and alteration.[6,7] The rocks cover the

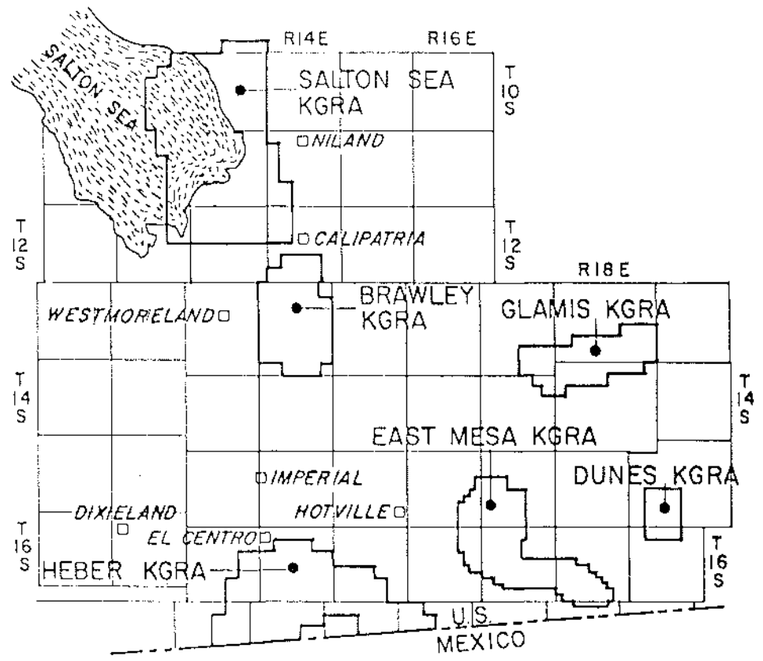

Fig. 1.
Location of some geothermal fields in the Imperial Valley.

spectrum from unaltered, unconsolidated sands, clays, and silts to highly indurated and altered sandstones, siltstones, and shales.

Various fields discovered in the Imperial Valley show large differences in formation-brine salinity, temperature, porosity, and permeability.[8] The two key factors in the commercialization of the fields are the salinity and temperature. Salinities in the area range from less than 2000 ppm at East Mesa to more than 300 000 ppm in the Salton Sea field. The temperature ranges from 160 to 320°C.

Extensive field and research reports have appeared in the literature on certain areas such as the East Mesa.[6-8] Information published about others such as the Brawley field is very limited.

Table II is a summary, comparing the characteristics of the different fields.

Studies of subsurface structure of sedimentary geothermal systems require mud log data, wireline logs, and core data. Generally the use of wireline logs to study the geothermal fields has been downplayed because of temperature limitation of existing tools or the inability to interpret the results. The limitation on interpolation is because of lack of adequate calibration data. Calibration facilities have recently become available.[9]

III. PURPOSE OF THE STUDY

This study was conducted to examine if the conventional well logs routinely run in geothermal wells can demonstrate any property indicative of the potential production zones. Furthermore, a comparison of the well log responses among various fields throughout the Imperial Valley was deemed desirable.

TABLE II

GENERAL INFORMATION ABOUT THE FIELDS UNDER STUDY

Field	Operator	No. of Wells	Salinity (ppm)	BHT (°C)
Brawley	Union Oil	10	200,000	260
East Mesa	U.S. Bureau of Reclamation	20	2,500	204
Heber	Chevron Resources	17	14,000	190
Westmoreland	Republic Geothermal, Inc.	6	20,000-70,000	260

Three major operators in the Imperial Valley agreed to furnish us with some limited amount of well logs. To protect the operators against the misuse of the data, the well logs were provided on the condition that we refrain from identifying the exact surface location and certain depth aspects of the wells.

It would have been highly desirable if the authors had had access to the complete suite of logs for all wells plus other available information such as drilling records, mud logs, and any core analyses. But in the absence of such complete data, it is believed that the limited information used here is still a significant step in developing an overall picture of the similarities and differences among the fields in the area.

It was fortuitous that all the logs received and used in this study were recorded by the same service company. Variations in the log data because of externally controlled parameters such as the properties of the drilling fluids, were normalized to compare the log-derived parameters.

IV. METHOD OF STUDY

The well logs were manually digitized for various computational purposes. For each well under study, a number of permeable beds throughout the entire depth column were selected for detailed studies and comparative evaluation.

The variation of certain log-derived values such as spontaneous potential (SP), gamma ray (GR), neutron porosity (ϕ_N), resistivities of the deep induction log (R_{ILD}) and Laterolog 8 (R_{LL8}) were statistically analyzed, and the mean values were plotted on spiderweb diagrams. The diagrams were arranged according to the depth of the permeable sections.

Several cross plots were prepared to study certain characteristics of the permeable sections from two independently measured parameters. These cross plots included the cross plots of both R_{ILD} and R_{LL8} vs ϕ_D and ϕ_D vs ϕ_N.

The procedure of computing $(Q_v)_{sand}$ was applied to the digitized parameters, and attempts were made to determine the depth profile of the cation exchange capacity per unit volume of the permeable zones.

Finally, the well logs were scrutinized for detection of unusual effects on various recorded parameters. Included in this aspect of study were the reversal of position of R_{ILD} with respect to R_{LL8}, excessive or

negative correction on the density logs, and borehole problems as evident from the caliper log.

V. REVIEW OF LOG-DERIVED PARAMETERS

Before the well logs were digitized for computational aspects of the study, a quality check was made as to the acceptability of the furnished information. Using various overlays, repeat sections, and the calibration check, the well logs were found to be generally of good quality with some exceptions where tool problems prevented the recording of some curves beyond a certain depth. Oftentimes, the temperature-related problems prevented the continuous recording of resistivity or other curves.

VI. ANALYSIS OF WELL LOG DATA

As indicated before, the purposes of this study were first to see the similarities among the well logs from various fields of the Imperial Valley and second to establish the features on the logs that infer the presence of hydrothermal zones.

In terms of correlation across the Valley, the spiderweb diagrams were used to observe general trends of various parameters with depth. These trends for different fields are summarized in Table III.

In general, the features common among various fields include the following:

- increase of the R_{LL8} with depth,
- increase of the R_{ILD} with depth, and
- decrease of ϕ_N and ϕ_D with depth.

TABLE III

SUMMARY OF WELL LOG RESPONSES AS DEPTH INCREASES

Well	R_{LL8}	R_{ILD}	R_{sand}/R_{shale}	ρ_{sand}/ρ_{shale}	ϕ_N	ϕ_D	R_w from Cross Plot
Mesa 6-1	increase	increase	≤ 1	< 1	decrease	decrease	decrease
Brawley A	increase	increase	≥ 1	< 1	decrease	decrease	increase
Brawley B	increase	increase	> 1	< 1	decrease	constant	increase
Heber A	increase	increase	> 1	< 1	decrease	decrease	constant
Heber C	increase[a]	increase[a]	> 1	≤ 1	decrease[a]	decrease	decrease
Westmoreland 2	increase	increase	> 1	< 1	decrease[a]	decrease[a]	increase
Westmoreland 3	increase	increase	< 1	< 1	decrease	decrease	decrease

[a] Change in direction is noted.

Figures 2-5 show these typical trends for well Heber A. The depth trend of other log-derived values such as SP and GR have shown inconsistencies among the different fields.

The next phase of this study focuses on the explanation of these trends. The loss of electrical conductivity with depth may be caused by one or the combination of the following:

- a drop in the formation-brine salinity,
- a drop in formation porosity, and
- a drop in surface conductivity of clays.

The possibility of a drop in formation-brine salinity with depth can be ruled out on some wells when checked against the field evidence of high-salinity fluids from these fields. These can also be verified by studying the resistivity-porosity cross plots for various wells. Wells Mesa 6-1, Heber C, and Westmoreland 3 indicate lower R_w's for deeper sands. Other wells such as Brawley A, Brawley B, and Westmoreland 2 show evidence of an increasing trend in R_w with depth. Heber A shows relatively constant R_w depth profile. Figures 6-8 show some typical resistivity-porosity cross plots.

While the change in R_w may be responsible for the resistivity increase on some logs, its contribution to the overall change lessens when one considers the behavior of the R_{LL8}. For example, as shown in Fig. 9, Mesa 6-1 from a cross plot of R_{LL8} vs ϕ_D shows uniform R_{mf} with depth, while both R_{LL8} and R_{ILD} increase with depth. Since for this well R_w decreases with depth, the cause of formation-resistivity increase must be the other two factors, namely, a decrease in porosity or a decrease in the surface conductivity of formation. Similar observations can be made with respect to Heber C and Westmoreland 3. Some exceptions ae Brawley A, B, and Heber A. But the same process affecting Mesa 6-1, Heber C, and Westmoreland 3 may have affected the others.

To examine the changes in porosities with depth, depth plots of ϕ_D and ϕ_N were made for individual wells. All wells indicate a definite drop in porosity as recorded from both the density log and the neutron log. Figures 10-11 show such typical trends for well Brawley A. The indicated drop of porosity alone can account for the increase in R_{LL8} and R_{ILD} with depth regardless of changes in R_w. We must examine the cause and the nature of the porosity reduction with depth as this results in some clues for subsurface exploration of hydrothermal zones.

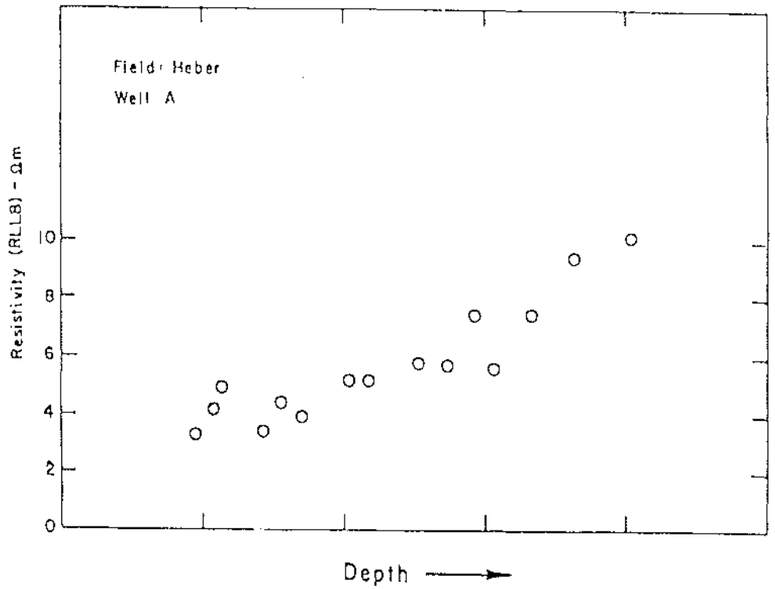

Fig. 2.
Heber A - R_{LL8} vs depth.

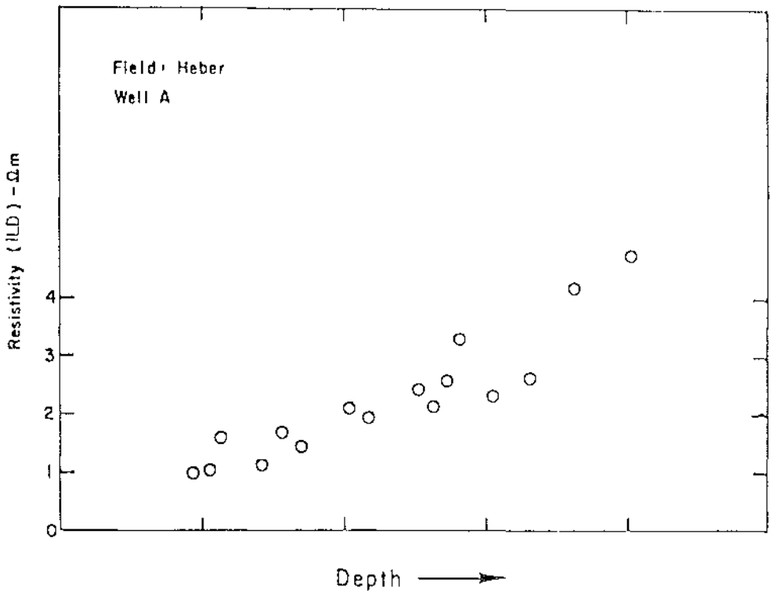

Fig. 3.
Heber A - R_{ILD} vs depth.

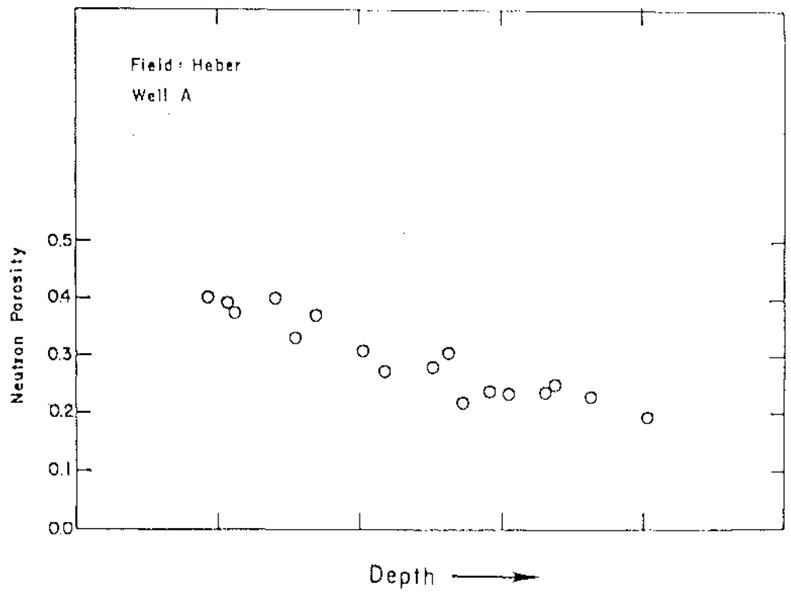

Fig. 4.
Heber A - ϕ_N vs depth.

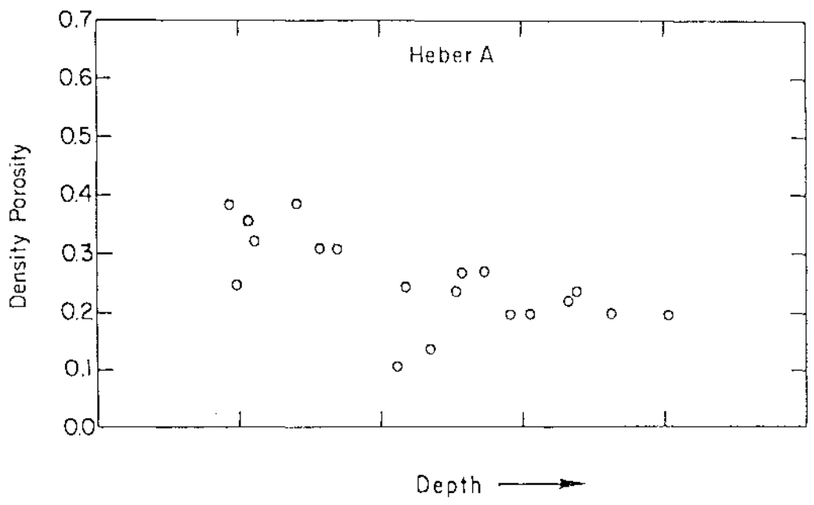

Fig. 5.
Heber A - ϕ_D vs depth.

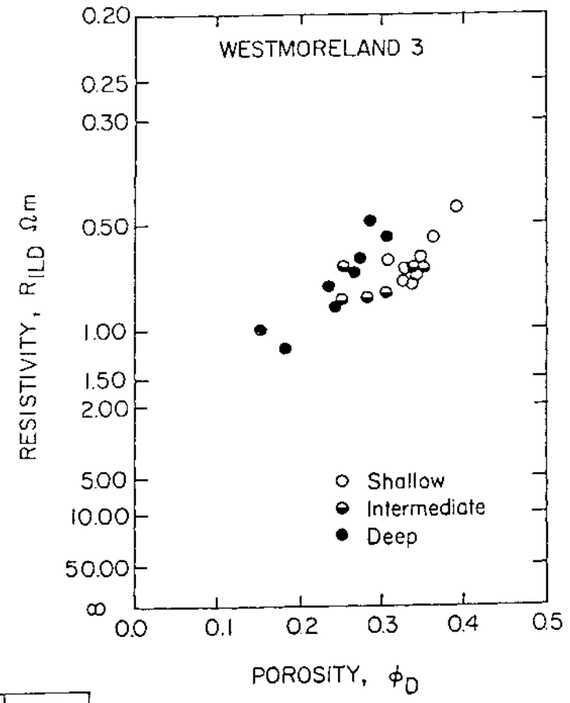

Fig. 6.
Westmoreland 3 - R_{ILD} vs ϕ_D.

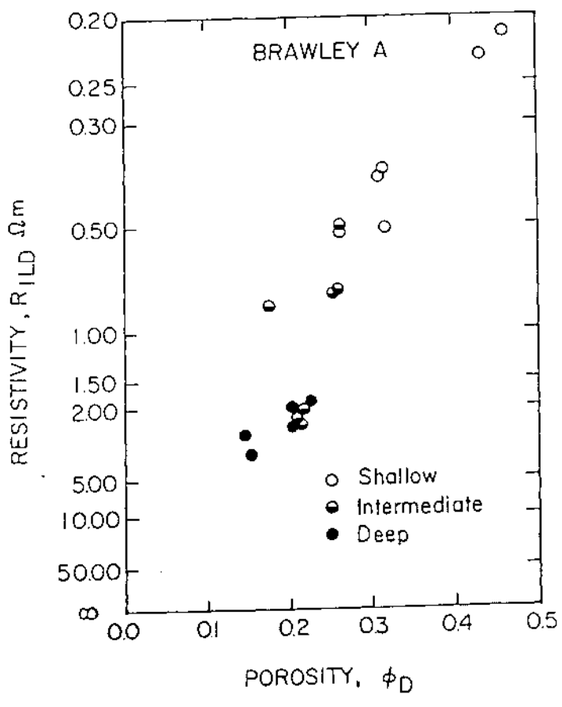

Fig. 7.
Brawley A - R_{ILD} vs ϕ_D.

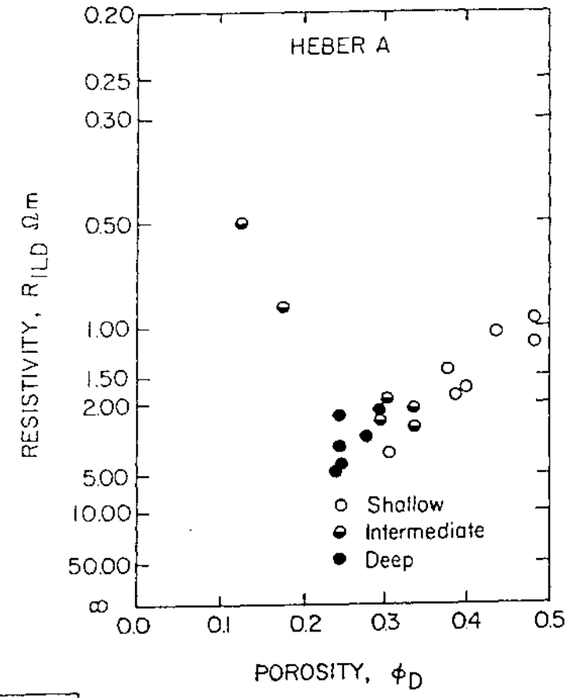

Fig. 8.
Heber A - R_{ILD} vs ϕ_D.

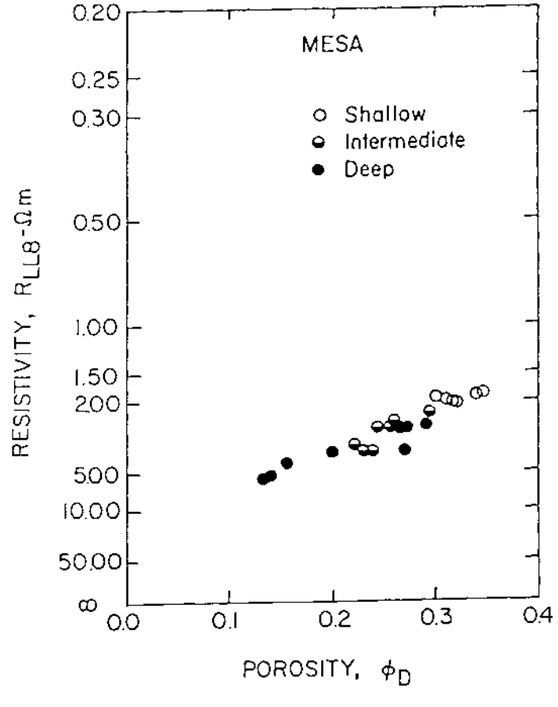

Fig. 9.
Mesa 6-1 - R_{LL8} vs ϕ_D.

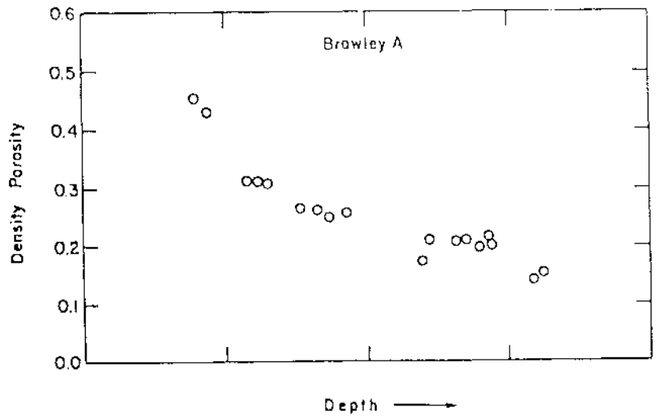

Fig. 10.
Brawley A - ϕ_D vs depth.

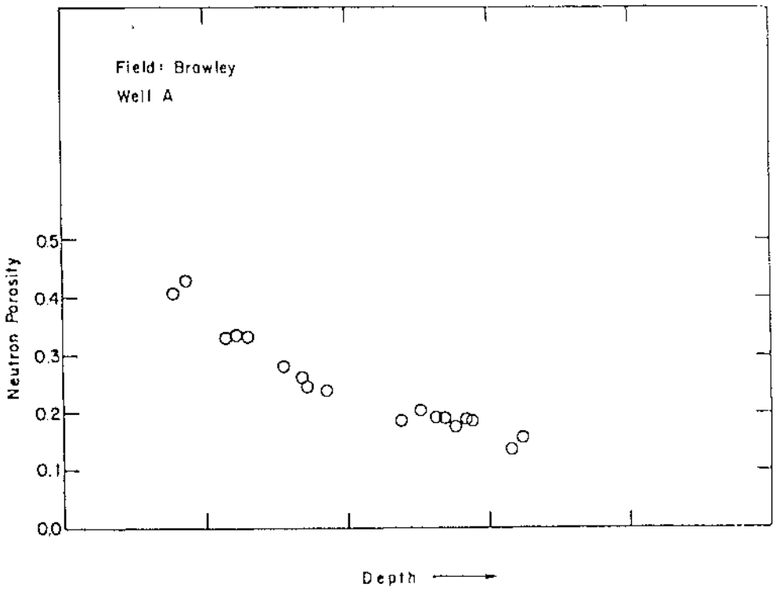

Fig. 11.
Brawley A - ϕ_N vs depth.

If the drop is merely a reflection of sediment compaction with depth, both the ϕ_D and ϕ_N must show porosity reduction while the $\phi_N > \phi_D$ relationship is maintained because of the shaly nature of the original sediments. But as shown in Figs. 12 and 13 for wells Brawley A and Heber C, the cross plots of ϕ_D vs ϕ_N indicate that a line with a unit slope can represent the data points for the deep formations. This means the loss of bound water for the formation. The loss of bound water can be attributed to thermal alteration of clays. These alterations happen if hydrothermal fluids have found their way through the permeable beds to affect the various constituents of the rock.

The loss of bound water and the apparent absence of active clays can also account for the loss of surface conductivity and thus an increase in formation resistivity.

It is interesting to note that the plots of R_{sand}/R_{shale} correlate very well with the observation made earlier with respect to the changes of R_w with depth. For all cases where the cross plots indicate an increase of R_w with depth, R_{sand}/R_{shale} ratios also increase with depth. Figure 14 is an example for Brawley B. For wells such as Mesa 6-1 and Westmoreland 3 when a decrease of R_w with depth was evident from the cross plot, R_{sand}/R_{shale} decreases with depth. Figure 15 shows the plot for Westmoreland 3. This observation points out the nature of the invading brines in the permeable sections and provides a comparison with the original brine of the sedimentary column trapped in the shales. This ratio change, because of salinity variation, is further confirmed when the relationship of $(\rho_b)_{sand}$ and $(\rho_b)_{shale}$ is examined on various logs. As shown in Figs. 16-17, this bulk-density ratio is less than unity indicating the salinity change above is the cause of increasing or decreasing the trend in R_{sand}/R_{shale}.

As a further check, the procedure for estimating Q_v profile[10] with depth was employed here, and the results for Brawley B and Westmoreland 2 are shown in Figs. 18-19. In general, the patterns observed in the case of Cerro Prieto wells are not consistently seen here. This can be explained because either mineralogical differences exist between the formations studied here and Cerro Prieto or the inconsistencies observed on the SP log affect the computations.

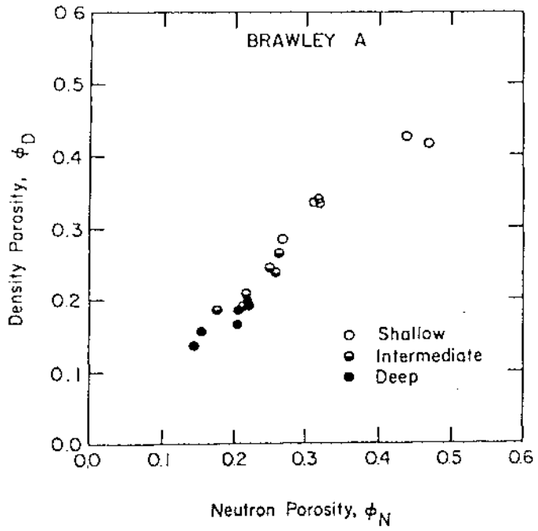

Fig. 12.
Brawley A - ϕ_D vs ϕ_N.

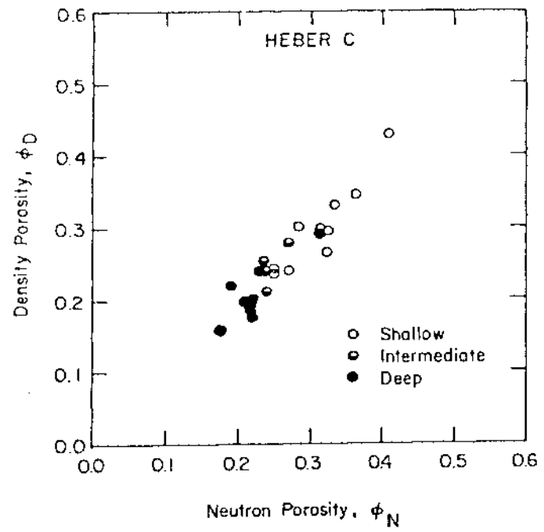

Fig. 13.
Heber C - ϕ_D vs ϕ_N.

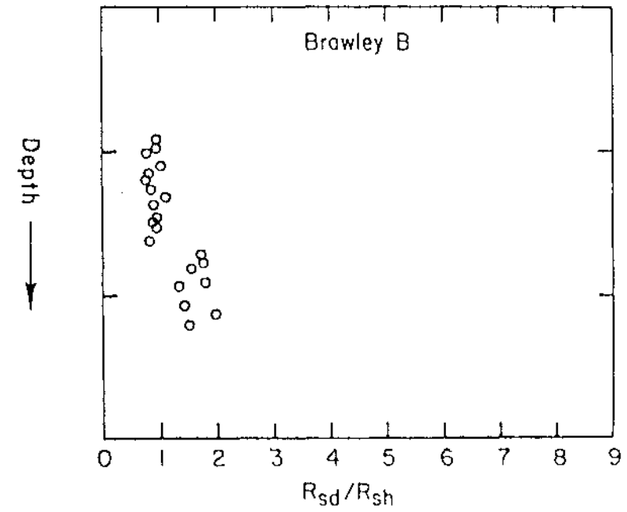

Fig. 14.
Brawley B - R_{sd}/R_{sh} vs depth.

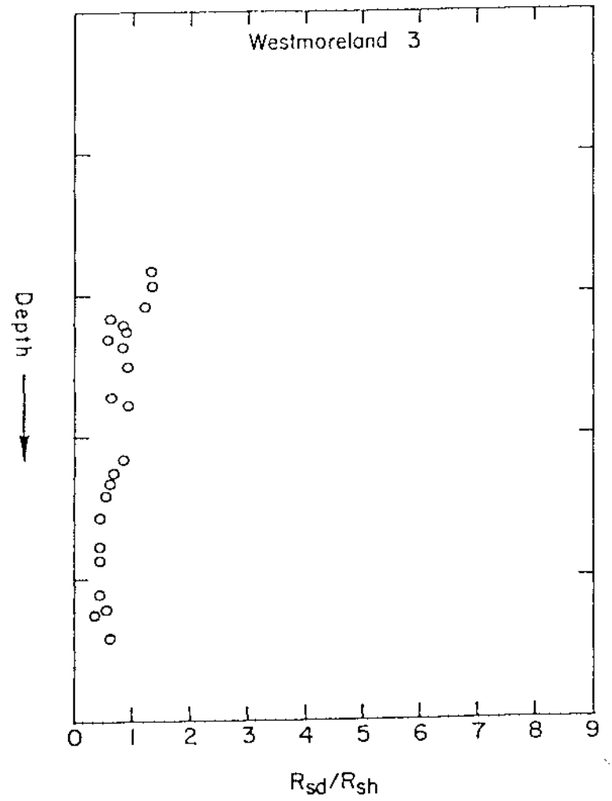

Fig. 15.
Westmoreland 3 - R_{sd}/R_{sh} vs depth.

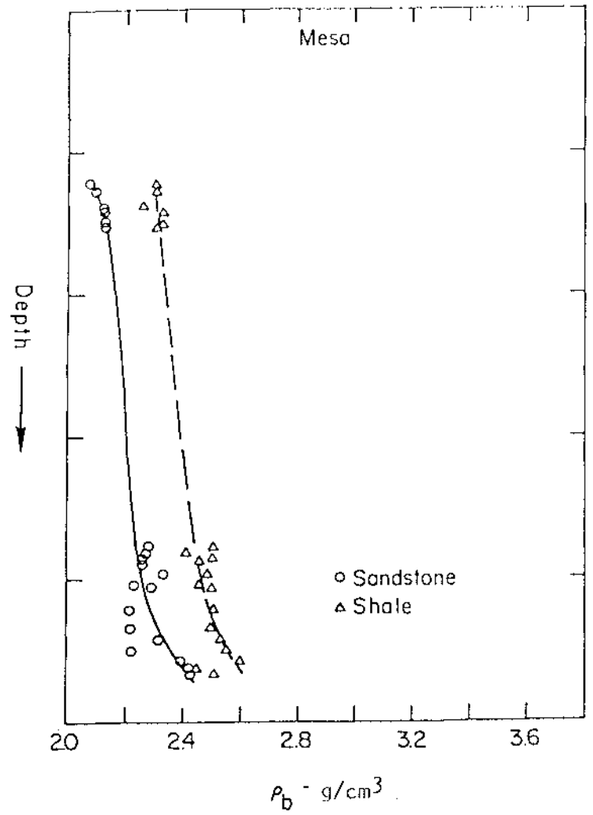

Fig. 16.
Mesa 6-1 - ρ_b vs depth.

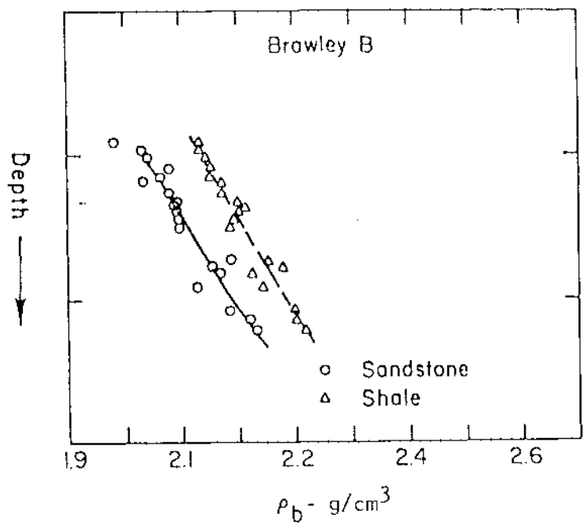

Fig. 17.
Brawley B - ρ_b vs depth.

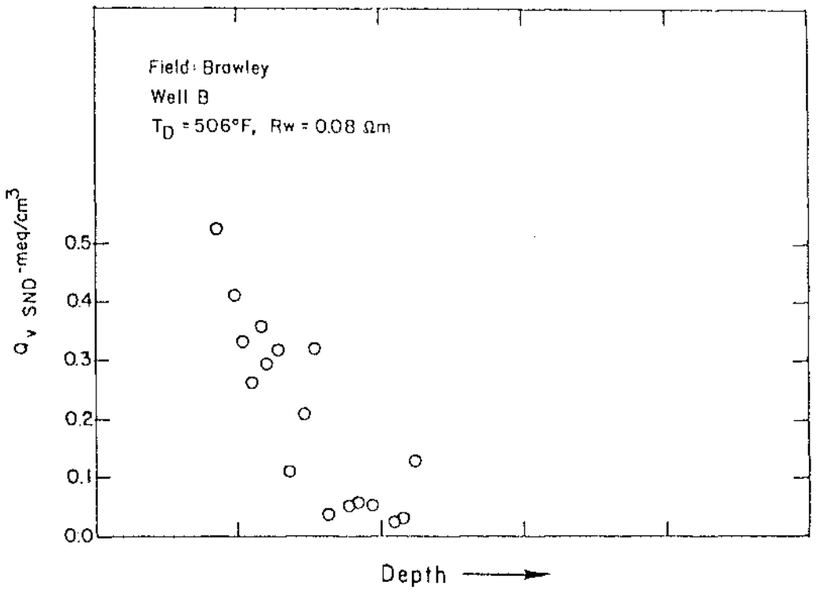

Fig. 18.
Brawley B - Q_V vs depth.

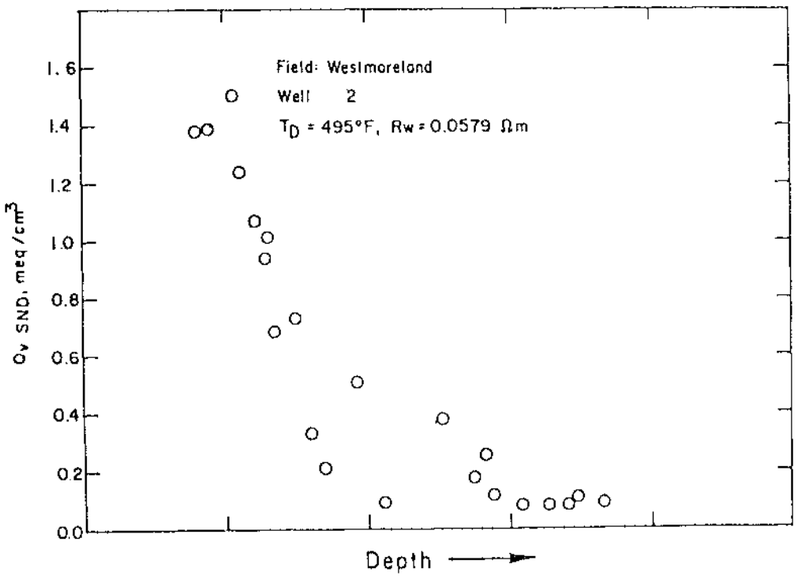

Fig. 19.
Westmoreland 2 - Q_V vs depth.

The effect of hydrothermal alteration on both the ϕ_N - ϕ_D cross plots and the resistivity changes with depth are remarkable. The effect on resistivity alone was checked experimentally where samples of a typical clay containing rock (Berea sandstone) were subjected to boiling under high pressure and temperatures. Under a condition of 300°C and 183 kPa, a significant drop in rock electrical conductivity was observed. The details are discussed in the Appendix, and some of the results are shown in Table IV. A brine-saturated rock with a Q_v of 0.21 meq/mℓ can lose 21% of its electrical conductivity by exposure to high-temperature brine. Unfortunately, we were not equipped to see the changes in ϕ_N losses due to boiling, but this is an area for further research.

VII. EFFECT OF PYRITE CONTENT AND FRACTURES

Some studies published on the mineralogy of the formations in the Imperial Valley point out the existence of pyrite in the rocks.

The effect of pyrite (F_eS_2) on log-derived parameters has been studied by Clavier et al.[11] The presence of pyrite causes significant changes in the measured bulk density and the resistivity from the induction log.

Since the formation-water salinity is higher than the salinity of the mud filtrate, the relationship of

$$C_w > C_{xo}$$

is expected to be true at all times. The presence of pyrite, if any, will tend to exacerbate the above relationship.

A review of the induction electric logs for the Imperial Valley wells shows no deviation to this condition except for two wells in the Westmoreland area. This is the only case where the response of the deep induction logs

TABLE IV

EXPERIMENTAL RESULTS ON RESISTIVITY AND Q_v CHANGES OF BEREA ROCK WITH BOILING

	Resistivity, Ωm, before boiling	Resistivity, Ωm, after boiling		Q_v meq/mℓ of PV	
Core		Measured	Calculated by Eq. (A-1) (without BQv)	Resistivity Method	Chemical Method
#1	2.506	3.200	2.8300	0.21353	0.20763
#2	2.7140	3.667	3.1332	0.1462	0.1223
#3	1.5630	1.8755	1.8013	0.05744	0.1056

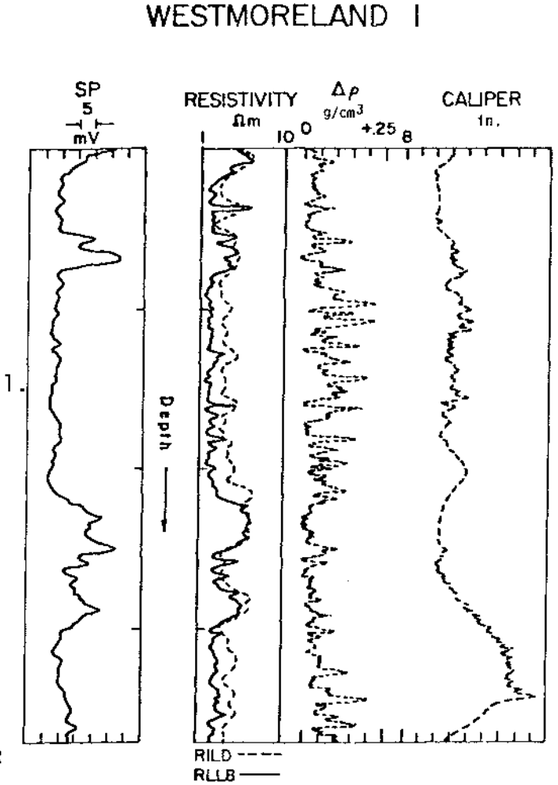

Fig. 20.
Resistivity reversal in Westmoreland 1.

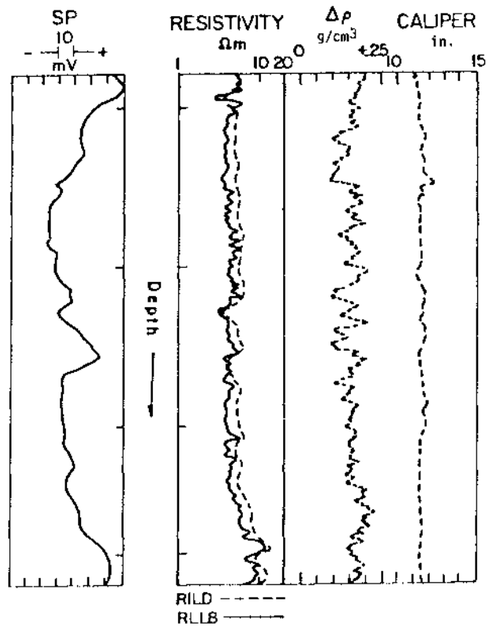

Fig. 21.
Resistivity reversal in Westmoreland 2.

indicates lower conductivities than those obtained from Laterolog 8, Figs. 20 and 21.

The major causes of this reversal are the salinity reversal between formation fluid and mud filtrate or the possible existence of vertical fractures. The proximity of the well to the Salton Sea area and the information on the log heading with respect to the mud resistivities preclude the assumption of salinity reversal. The presence of fracture needs further analyses, since the resistivity reversal has not been observed in other wells.

VIII. SUMMARY AND CONCLUSIONS

Review of the well logs from certain geothermal fields in the Imperial Valley, California, indicates that there are similarities among various recorded parameters. Among these are the typical depth profiles of resistivities and porosities, indicating a loss of both effective and noneffective porosities caused by hydrothermal alterations.

Cross plots of resistivity from deep induction log vs ϕ_D were found to serve as a convenient method for detecting salinity changes with depth. The loss of electrical conductivity with depth is also a clue when the target zones are approached. Such zones are further characterized by cross plots of $\phi_N - \phi_D$ where the loss of bound water results in clustering of the points along a unit slope line. Problems with recorded SPs precluded the widespread application of Q_v depth profile.

ACKNOWLEDGMENTS

The authors are indebted to Mark Mathews for his support and encouragement throughout the study.

The assistance from the managements of Union Oil Co. of California, Chevron Resources, and of Republic Geothermal in providing the copies of the well logs is greatly appreciated.

REFERENCES

1. Ershaghi, I., Ghaemian, S., and Abdassah, D., "Lithology and Hydrothermal Alteration Determination from Well Logs for the Cerro Prieto Wells, Mexico," Los Alamos National Laboratory report LA-9075-MS (October 1981).

2. Elders, S. A., Rex, R. W., Meidav, T., Robinson, P. T., and Biehler, S., "Crustal Spreading in Southern California," Science 178, 15-241 (1972).

3. Hoagland, J. R., "Petrology and Geochemistry of Hydrothermal Alteration in Borehole Mesa 6-2, East Mesa Geothermal Area, Imperial Valley, California," M.S. thesis, University of California Riverside (1976).

4. Biehler, S., Kovach, R. L., and Allen, C. R., "Geophysical Framework of the Northern End of the Gulf of California Structural Province," in Marine Geology of the Gulf of California: American Association of Petroleum Geologists, Memoir 3, 126-143 (1964).

5. Brook, C. A., Mariner, R. H., Mabey, D. R., Swanson, J. R., Guffanti, M., and Muffler, L. J. P., "Hydrothermal Systems with Reservoir Temperatures <90°C," in Assessment of Geothermal Resources of the United States - 1978, U.S. Geological Survey Circular 790, 48 (1979).

6. Miller, K. R. and Elders, W. A., "Geology, Hydrothermal Petrology, Stable Isotope Geochemistry, and Fluid Inclusion Geothermometry of LASL Geothermal Test Well C/T-1 (Mesa 31-1), East Mesa, Imperial Valley, California, U.S.A.," Los Alamos Scientific Laboratory report LA-8515-MS (September 1980).

7. White, D. E. and Muffler, L. J. P., "Metamorphism of Upper Cenozoic Sediments to Greenschist Mineral Assemblages; Salton Sea Geothermal Area, California," Geological Society of America, Special Paper 82 (1964).

8. Anderson, D. N., "The Most Promising Geothermal Fields in the Western United States," presented at the Geothermal Resources Council, Short Course No. 10, Anaheim, California (March 25-26, 1981).

9. Mathews, Mark, "Calibration Models for Fractured Igneous Rock Environments," paper L, SPWLA Transactions (1980).

10. Ershaghi, I. and Ghaemian, S., "Estimation of Q_v Profile in a Sedimentary Type Geothermal Reservoir," SPE 9927, presented at the 1981 California Regional Meeting of SPE, Bakersfield, California (March 25-26, 1981).

11. Clavier, C., Heim, A., and Seala, C., "Effect of Pyrite on Resistivity and Other Logging Measurements," paper HA, SPWLA Seventeenth Annual Logging Symposium Transactions (June 9-12, 1976).

APPENDIX

EXPERIMENTAL STUDIES OF Q_v MEASUREMENT

In an effort to study the changes in the Q_v properties of clay containing rocks when subjected to high-temperature conditions, a series of experiments were conducted. These experiments consisted of measurement of Q_v before and after hydrothermal alteration by both the titration method and resistivity measurements.

Core materials used were of the Berea sandstone type selected for this study because of their homogeneous characteristics. The samples used had porosities ranging from 19 to 26% and permeabilities of 60 to 500 md.

The hydrothermal alteration was imposed on the cores by boiling them in a pressurized vessel up to a temperature of 300°C for 24 hours. The brine used was 5% NaCl.

To measure the Q_v of the samples before the hydrothermal effects, the resistivities of the saturated cores were measured and compared to the computed resistivities assuming no clay content ($C_o = C_w/F$). From the difference between the two measurements, a value for Q_v was obtained from the Waxman-Smits equation

$$C_o = \frac{1}{F}(BQ_v + C_w) \qquad \text{(A-1)}$$

where

$$F = \frac{0.625}{\phi^{2.15}},$$

$$B = [1-0.86 \exp(-C_w/0.02)]0.001\, \lambda^e_{Na},$$

$$\lambda^e_{Na} = 38.3 \text{ cm}^2 \text{ equiv}^{-1}\text{ohm}^{-1},$$

Q_v = meq/mℓ of PV, and

C_o, C_w = mho cm^{-1}.

The Q_v's were also measured from the titration method where the core samples were flooded by 0.1 N NH_4A_c solution. The effluent was then analyzed in a Kjeldahl flask for ammonium content. The difference in NH_3 concentration corresponding to the boiled and unboiled core was used to estimate the Q_v of the core. The results of the experimental data obtained on some core samples are shown in Table IV.

☆U.S. GOVERNMENT PRINTING OFFICE: 1984-0-776-026/4049

Printed in the United States of America
Available from
National Technical Information Service
US Department of Commerce
5285 Port Royal Road
Springfield, VA 22161

Microfiche (A01)

Page Range	NTIS Price Code	Page Range	NTIS Price Code	Page Range	NTIS Price Code	Page Range	NTIS Price Code
001-025	A02	151-175	A08	301-325	A14	451-475	A20
026-050	A03	176-200	A09	326-350	A15	476-500	A21
051-075	A04	201-225	A10	351-375	A16	501-525	A22
076-100	A05	226-250	A11	376-400	A17	526-550	A23
101-125	A06	251-275	A12	401-425	A18	551-575	A24
126-150	A07	276-300	A13	426-450	A19	576-600	A25
						601-up*	A99

*Contact NTIS for a price quote.